Severine Le Faucheur   ORCID iD: 0000-0002-9985-2435

Laderriere et al.

Temperature and photoperiod affect biofilm response to Ni

Temperature and Photoperiod Affect the Sensitivity of Biofilms to Nickel and its Accumulation

Vincent Laderriere,[1]*0000-0002-9985-2435 Maxime Richard,[1] Soizic Morin,[2]

Séverine Le Faucheur,[3] and Claude Fortin[1]

[1] Institut National de la Recherche Scientifique, Centre Eau Terre Environnement, 490 rue de la Couronne, Québec, Canada

[2] Institut national de recherche pour l'agriculture, l'alimentation et l'environnement, EABX, 50 avenue de Verdun, Cestas, France

[3] Université de Pau et des Pays de l'Adour, IPREM, 2 avenue Pierre Angot, Pau, France

Correspondence Vincent Laderriere, Institut National de la Recherche Scientifique, Centre Eau Terre Environnement, 490 Rue de la Couronne, Québec, Quebec G1K 9A9 Canada

8/2/21; 10/25/21; 3/23/22

Abstract: While metal impacts on fluvial communities have been extensively investigated, effects of abiotic parameters on community responses to contaminants are poorly documented. Variations of photoperiod and temperature commonly occur over the course of a season and could affect aquatic biofilm communities and their responses to contaminants. The objective of this study was to characterise the influence of environmental conditions (photoperiod and temperature) on Ni

bioaccumulation and toxicity using a laboratory-grown biofilm. Environmental

parameters were chosen to represent variations that can occur over the summer

season. Biofilms were exposed for 7 days to six dissolved Ni treatments (ranging from

6 to 115 μM) at two temperatures (14°C and 20°C) using two photoperiods (16/8 and

12/12 light/dark cycle). Under these different scenarios, structural (dry weight

biomass, chlorophyll-a) and functional biomarkers (photosynthetic yield and Ni

content) were analysed at four sampling dates allowing us to evaluate Ni sensitivity of

biofilms over time. The results highlight the effects of temperature on Ni

accumulation and tolerance of biofilms. Indeed, biofilms exposed at 20°C

accumulated 1.6 to 4.2-fold higher concentrations of Ni and were characterized by a

lower EC50 value using photosynthetic yield as compared to those exposed at 14°C.

Regarding the photoperiod, significantly greater rates of Ni accumulation were

observed at the highest tested Ni concentration for biofilms exposed to a 12/12

compared to 16/8 light/dark cycle. Our study demonstrates the influence of the

temperature on biofilm metabolism and illustrates that environmental factors may

influence Ni accumulation response and thus, Ni responses of phototrophic biofilms.

INTRODUCTION

Freshwater biofilms are a complex assemblage composed of eukaryotic (*e.g.*, microalgae, fungi, protozoa) and prokaryotic (*e.g.*, bacteria, cyanobacteria) microorganisms living encapsulated in a polysaccharide matrix and growing on submerged substratum surfaces (Flemming & Wingender, 2010; Battin et al., 2016). These communities are at the basis of aquatic trophic chains and are fundamental to energy flow, nutrient cycling and global biogeochemical fluxes (Battin et al., 2016). Moreover, they are known to respond rapidly to physicochemical or environmental stress while being able to tolerate those stresses over extended periods of time (Guasch et al., 2016; Hobbs et al., 2019). Therefore, due to the known potential for periphytic biofilms to accumulate contaminants, they are likely to influence the fate of metals in freshwater ecosystems, which makes them particularly interesting for contamination assessment studies (Hobbs et al., 2019; Bonnineau et al., 2020; Mebane et al., 2020).

Metals are naturally present in freshwater ecosystems but many anthropogenic activities represent significant sources of releases into aquatic environments (*e.g.* agriculture, mining, urbanization, etc; Lavoie et al., 2012; Faburé et al., 2015). In this context, biological communities are exposed to multiple stresses and periphytic biofilms have been pointed out as promising bio-indicators of the effects of contaminants such as metals on aquatic systems (Guasch et al., 2016). For instance, because biofilms are at the base of the food chain, they can be used as a proxy of the transfer of contaminants through the trophic chain (Mebane et al., 2020). Several studies investigated the direct or indirect effects of metals on relationships between biofilms and various consumers including micro/macrofauna or fish (Namba et al., 2020). Furthermore, Chl-a fluorescence (Corcoll et al., 2011), diatom assemblages

(Lavoie et al., 2012), antioxidant enzymes activities (Bonet et al., 2013), photosystem II photochemistry (Lambert et al., 2016) and fatty acid composition (Fadhlaoui et al., 2020) are all markers of contaminant effects which can be used with biofilms. Among markers, metal accumulation in periphytic biofilms has been shown to be a robust indicator of exposure (Ancion et al., 2010; Leguay et al., 2016; Laderriere et al., 2020). Some metals have been extensively studied, such as Cu (Morin et al., 2017; Pesce et al., 2018), Zn (Corcoll et al., 2012; Lavoie et al., 2012), or Pb (Ancion et al., 2010; Stewart et al., 2015), whereas others like Ni have been poorly examined (Bonnineau et al., 2020). Nickel is often associated geochemically with other metals (*e.g.* iron, cobalt, copper), therefore soils with a high concentration of these elements generally contain large amounts of Ni (Harasim & Filipek, 2015). Due to the intrusive nature of extraction and processing techniques, Ni- producing countries such as Indonesia, Philippines, New Caledonia and Canada have reported high levels of environmental contamination (Gillmore et al., 2021). As an example, concentrations of Ni in surface waters have been shown to be high due to mining and metallurgical activities within regions of the Canadian provinces of Ontario (Lavoie et al., 2018) and Quebec (Leguay et al., 2016; Laderriere et al., 2020).

In aquatic environments, characterizing the interactions between metals and living organisms can be challenging. For example, accumulation is a dynamic process that is influenced by a multitude of factors, many of which can experience diurnal, daily and seasonal variations, such as nutrient concentrations or flow conditions (Serra et al., 2010; Chaumet et al., 2019; Tlili et al., 2020). Metal speciation (e.g. metal binding by dissolved ligands such as organic matter) is known to determine the bioavailability of these contaminants, and subsequently their uptake (Tercier-Waeber et al., 2012). It is difficult to quantify the impact of natural environmental variables on the fate and

behaviour of toxicants, especially in the context of a changing climate. Ecotoxicologists are challenged with predicting how environmental factors will affect the response of toxic substances at the individual or the community level (Moe et al., 2013). Environmental conditions, such as temperature (Lambert et al., 2016; Morin et al., 2017; Pesce et al., 2018) or incident light characteristics (Cheloni & Slaveykova, 2018; Chaumet et al., 2020), are known to directly influence aquatic organisms, but also indirectly by modifying physicochemical parameters of the aquatic media. More specifically, Lambert et al. (2016) and Pesce et al. (2018) showed that the bioaccumulation of Cu was reduced at higher temperatures. Therefore, changes in temperature and light conditions may alter metal toxicity. Better understandings of the mechanisms driving trace metal effects in association with environmental factors such as light and temperature will reduce the uncertainties associated with the extrapolation of laboratory data to the natural environment and possibly integrate site-specific conditions in risk assessment.

In a previous study, we found that biofilm metal content was consistent over large geographical scales and in different types of ecosystems (Laderriere et al., 2021). However, some differences in regression slopes observed between free metal ions and biofilm metal concentrations were found between the different studied regions. It was hypothesized that environmental factors could explain the differences of metal accumulation concentrations in biofilms. The aim of the present study was to evaluate if seasonal variability could modify Ni accumulation by periphytic biofilm in the perspective of using the internalized concentration as a biomarker of metal contamination in surface waters. The experiments were designed to identify the possible effects of temperature and photoperiod variations in biofilm metal accumulation and tolerance. Variations in temperature and photoperiod were chosen

to represent daily or seasonal variations. For this purpose, natural river biofilms were collected on a site free of metal contamination and cultivated in the laboratory before subsequent experiments. Biofilm characterization, Ni-induced toxicity, metal accumulation and environmental parameters (including metal contamination levels) were monitored.

MATERIALS AND METHODS

Biofilm culture

Natural biofilms were collected from the Cap-Rouge River near Quebec City by scraping several rocks with a toothbrush. This river was chosen due to its low metal concentrations, with Ni and other metal concentrations near or less than 0.01 μM (see supporting information for the physico-chemistry of the Cap-Rouge River Table S1). Biofilms were resuspended in river water to form a periphytic homogenate, which was used to inoculate a recirculating laboratory culture channel (Volume: 60 L; Length: 40 cm, Width: 20 cm, Height: 12 cm; plexiglass). Unglazed ceramic tiles (surface of 23 cm^2) were placed at the bottom of the channel as growth substrate and Fraquil medium was used as a culture medium (see supporting information for Fraquil medium composition; Table S2). A submersible pump (capacity of 4350 L/h; PC1150; BASIN+) placed in a 40-L bucket was used to maintain a continuous flow, to provide oxygenation and to simulate a riffle environment. Biofilms were cultivated under controlled light intensity (approximately 70 to 80 μmol·photon/m^2/s) with a light/dark photoperiod of 16/8 and temperature (14°C) in an environmental chamber for a period of approximately 35 days prior to exposure experiments. During this culture period, biofilms were grown without any harvesting and the absence of grazers was checked. The biofilm cultures used for the exposures were therefore not in an early growth phase.

Biofilm exposure experiments

Three independent experiments were performed, at two light/dark photoperiods (16/8 or 12/12) and two temperatures (14 or 20°C) in order to mimic different conditions occurring within summer. The combination of experiments is therefore focusing on first, a variation of photoperiod and second, a variation of temperature. The light intensity was maintained between 70 to 80 µmol·photon/m^2/s for all experiments. The condition at 14°C with a light/dark photoperiod of 16/8 was defined as reference for comparison. Biofilms were acclimated to the studied light/temperature conditions for two weeks prior Ni-exposure in order to avoid an abrupt change in temperature and light, which rarely occurs in the environment. The different exposure experiments were carried out one after another, leaving a two-week period between each experiment to allow for the acclimation of the biofilm to the modified environmental conditions. After these 2-week periods, the Ni exposures were performed over 7 days. Before each Ni exposure, 144 tiles were randomly selected from the culture channel and placed in the 12 exposure channels. A total of 12 tiles were placed in each unit allowing for 3 pseudo-replicates per exposure channel for each sampling date.

The experimental setup (Figure 1) was composed of twelve independent exposure channels (volume: 6 L; length: 100 cm, width: 20 cm, height: 10 cm; plexiglass). Each unit was independently supplied with recirculating Fraquil medium at a pH of 6.9 ± 0.1 with a submersible pump (capacity of 454 L/h; Laguna) placed in a 10 L plastic bucket to ensure a continuous circulating medium. Six Ni treatments were tested: one control (0 µM of total Ni) and five different total Ni concentrations (6, 10, 30, 60 and 120 µM Ni). Exposure solutions were prepared from a Ni stock solution (ICP standard solution of 10 g/L of Ni in 4% HNO$_3$ (v/v); SCP Science). For each treatment, two

independent microcosms were assigned. Before each experiment, all units as well as their buckets, pipes and pumps were pre-washed with 10% nitric acid ACS grade (v/v; Fisher Scientific). The water circulation in all exposure units was initiated 24 h before the tiles covered with biofilm were put in place, allowing the exposure medium to equilibrate. No change of water was made during each exposure and experiments were carried out for seven days, with four sampling times (0, 1, 4 and 7 days). The first sampling time (t_0) was done before Ni addition in the different exposure channels. This time thus allowed to obtain the inter-channel variability before the appearance of Ni effects on biofilms by its addition in the culture medium. Water and biofilm samples were collected at each sampling time, along with in-situ measurements of pH and temperature by a multi-parametric probe (Orion Star A220; ThermoFisher Scientific).

In order to simplify the comparison of the different tested conditions of temperature and light/dark cycle, we established the following code: T14P16 = 14°C in 16/8; T14P12 = 14°C in 12/12; and T20P16 = 20°C in 16/8. The combination of experiments T14P16 and T14P12 therefore focused on a variation of the photoperiod while experiments T14P16 and T20P16 allowed investigating the effect of temperature. In terms of water temperatures, each microcosm remained close to the target temperature with mean values of T14P16 = 14.4 ± 0.2°C, T14P12 = 14.8 ± 0.1°C and T20P16 = 19.3 ± 0.4°C (n = 48; one measure per microcosm and per sampling date).

Biofilm sampling and analysis

The three replicates of biofilm from each channel were sampled and prepared as described below. Biofilm was scraped from the top of one tile using a razor blade and collected in a large polypropylene tube (50 mL; Sarstedt). Biomass was then

resuspended in 10 mL of fresh Fraquil media and the homogenized solution was promptly divided for the different parameter analyses. From this volume, 4 mL was collected to measure Ni bioaccumulation and 3 mL to measure the photosynthetic yield and chlorophyll-a concentration.

In order to measure bioaccumulation, the 4 mL of resuspended biofilms were concentrated by removing the supernatant using a centrifugation step of 5 min at 6000 rpm. A volume of 10 mL of ethylenediaminetetraacetic acid (EDTA; 10 mM; pH 7) was then added to the pellets, vigorously shaken, and the centrifugation process was repeated after 5 min to eliminate the EDTA solution. The EDTA was used to distinguish adsorbed metals from intracellular contents (Hassler et al., 2004). The final pellets were kept in a freezer at −20°C before lyophilization for 48 h (Dura-Top/Dura-dry MP; FTS SYSTEMS). The dry biofilm was subsequently mineralized: 800 μL of HNO_3 (trace metal grade; Fisher Scientific) were added for 48 h and then 200 μL of H_2O_2 (optima grade; Fisher Scientific) were added for another 48 h. Finally, 800 μL of the digested biomass were diluted in 7.2 mL of ultrapure water (18 MΩ·cm) in a polyethylene tube (15 mL; Fisher Scientific) to reach 10% HNO_3 (v/v). All samples were kept at 4°C before subsequent analyses. Bioaccumulated Ni was measured by inductively coupled plasma–atomic emission spectrometry (ICP-AES; Varian Vista AX CCD). Certified reference material (IAEA- 450; algae) was analyzed to determine the efficiency of the digestion method (mean Ni recovery of 81.5 ± 0.5%; n = 3).

In order to measure the Ni induced toxicity on the phototrophic compartment of the biofilm, we used the effective photosynthetic activity as well as Chl-a concentration as biomarkers of effect. Effective photosynthetic activity (Photosystem II quantum yield; Φ_{PSII}) measurements were determined using a Pulse Amplitude

Modulated fluorimeter (Phyto-PAM; Heinz Walz GmbH; Germany) in quartz cuvettes, based on the average of three values per replicate and using the same methodology as described in Corcoll et al. (2012b). The Φ_{PSII} provides an estimate of the maximum efficiency of PSII photochemistry. Yields are presented on a relative scale ranging from 0 (no photosynthesis) to 1 (maximum) and values for biofilms are usually around 0.5 for undisturbed conditions. Measurements of all t_0 samples (before addition of Ni in the media) were used as a reference of photosynthetic yield. Time-response assessment of Ni chronic toxicity and effective concentration calculation were performed following the response of the Φ_{PSII} for each collection time using the control microcosms as a 100 % of efficiency at each collection time. Measurements were performed after 15 min of dark adaptation at room temperature and Φ_{PSII} was measured three times every 10 s until Φ_{PSII} values stabilized.

After measuring the Φ_{PSII}, samples were kept on ice before chlorophyll-a extraction. Samples were subsequently centrifuged at 5000 rpm for 5 min and the pellets were resuspended in 10 mL of 90 % acetone (v/v; Fisher Scientific). Pigments were extracted at 4°C during 12 h in the dark and then filtered onto GF/C filters (1.2 μM; Whatman). Pheophytin-corrected chlorophyll-a was determined spectrophotometrically (CaryEclipse; Varian) by measuring absorbance before and after acidification using 60 μL of HCl (ACS grade; Fisher Scientific; Steinman et al., 2006). Chlorophyll-a values were estimated by regression using the Phyto-PAM values ($R^2 = 0.92$, p-value < 0.001). Using the conversion factor between the surface of each tile (23 cm^2) and suspension volume used for the different descriptors, measured chlorophyll-a (Chl-a) values such as dry-weight biomass (DW) are expressed by the scraped surface (cm^{-2}). We also used the chlorophyll-a concentrations and dry-weight biomass to calculate the autotrophic Index (AI)

following the formula: *AI = DW (mg/cm²)/Chl-a (mg/cm²)* (Steinman et al., 2006).

This index provides information on the trophic status or relative viability of the biofilm community. An increase of the index suggests that the autotrophic community is decreasing with respect to the heterotrophic community.

Exposure medium analysis and Ni speciation

At each collection time and for each channel, two replicates of exposure medium samples were collected to measure the concentration of cations and model Ni speciation. To that end, a polypropylene syringe (20 mL; Fisher Scientific) was carefully rinsed three times with ambient media and used to filter exposure medium using polysulfonate filters (0.45 μm; VWR International). Samples were acidified to 10 % (v/v) HNO_3 (trace metal grade; Fisher Scientific) in a polyethylene tube (15 mL; Fisher Scientific) and stored at 4°C before subsequent analyses.

The concentrations of the constituent elements of the Fraquil medium such as cations (Ca, Mg, K, Na, P, Si) and metals (Cu, Co, Fe, Mn, Mo, Ni, Zn) were verified by ICP-AES in order to confirm nominal concentrations of nutrients and Ni. The Ni detection limit was 0.01 μM. Nickel speciation in Fraquil medium was calculated using MINEQL+ software at each sampling time. The software's default thermodynamic database was updated using the National Institute of Standards and Technology's Critically Selected Stability Constants of Metal Complexes database (v8.0). Chemical equilibrium modelling showed that Ni strongly bound to EDTA present (5 μM) in the Fraquil medium. As such, for a total Ni concentration lower than 5 μM, Ni was predominantly complexed by EDTA, whereas above 5 μM of total Ni, its main form was its free form with Ni^{2+} concentration, which could be approximated as follows: $[Ni^{2+}] = [Ni]_T - 5$ μM. A figure showing the major chemical

forms of Ni in the Fraquil medium as a function the total concentration in the medium is presented in the supporting information (see Figure S1).

Data and statistical analyses

Data were log-transformed before statistical analyses in order to satisfy the assumption of normality and homogeneity of variances. A p-value of 0.05 or less was considered significant. In order to test if there was a statistical difference between the two photoperiods and the two temperatures in terms of Ni accumulation, we determined least-squares estimates of the adjustable parameters of a Michaelis-Menten model (*i.e. Vm* and *K*) after 7 days of exposure (*nls* function; stats *package*; v4.0.4):

$$[Ni]_{Biofilm} = \frac{V_m \times [Ni^{2+}]}{K + [Ni^{2+}]}$$

The model had three levels of environmental conditions (T14P16, T14P12, T20P16) and thus the parameters *Vm* and *K* are specific for each temperature and photoperiod combination. Differences in models were tested using the *F*-test (*anova* function; stats *package*) by comparing the model when *Vm* and *K* are assumed to be identical for the three groups (*i.e.* environmental conditions) with the model for which both parameters vary from group to group. The difference between the estimated *Vm* and *K* of each environmental condition was tested using a t test (p-value adjusted with *Bonferroni* method) if a statistical difference in models was found. To model dose-response curves and extract effective concentrations (*drc* package; v 3.0.1), the Φ_{PSII} values measured at specific times were plotted against calculated free Ni concentrations. Dose–response curves were fitted to the data using the four-parameter log-logistic model. Calculated effective concentrations were compared between treatments using a t test (p-value adjusted with *Bonferroni* method). A linear discriminant analysis (LDA) was applied with every descriptor normalized by their

initial values (i.e. t_0 values; *ade4* package; v 1.7.16) in order to individualize data into similarly composed groups. All statistical analyses were performed with the R software (v4.0; https://cran.r-project.org).

RESULTS

Effects of temperature and light conditions on control biofilms

Dissolved Ni concentrations remained below the detection limit (*i.e.* 0.01 μM of dissolved Ni) throughout the experiments in control microcosms. Background Ni accumulation by control biofilms was detected with values ranging from 0.24 to 0.94 μmol/g dry weight. The highest values were measured in control biofilms exposed to the T14P12 conditions at day 4 (see supporting information; Table S4). However, except for that value, no statistical differences were found between exposure time within each condition. The internalized concentrations therefore remained stable with time. Figure 2 shows the time course of the biological parameters in the control biofilms (*i.e.* the two channels not exposed to Ni over the 7 days of experiment).

The biofilm dry weights varied amongst a single condition and increased with exposure time in particular in the T20P16 condition (Figure 2A). For this last condition, the biofilm biomass at the first sampling date (*i.e.* t_0) was already higher than at the end of the two other conditions and increased by a factor of 2.7 over time, highlighting the effect of temperature. Without distinction of sampling dates, the biomass means were 0.52 ± 0.09 mg/cm^2, 0.47 ± 0.18 mg/cm^2 and 1.32 ± 0.55 mg/cm^2 respectively for T14P16, T14P12 and T20P16. The biomass in the condition T20P16 was thus 2.6 and 2.8 times higher than those of T14P16 and T14P12, respectively. Similarly to biomass, Chl-a concentrations also show comparable values at T14P16 and T14P12 conditions, but 2.5 to 3.8-fold higher at T20P16 (Figure 2B). Average values were 40.5 ± 8.3 μg/cm^2, 49 ± 14 μg/cm^2 and 157 ± 16 μg/cm^2 for T14P16,

T14P12 and T20P16, respectively. However, if Chl-a concentrations only varied slightly over the 7 days of experiment in the T20P16 conditions, the two other conditions showed an increasing trend by a factor of 2. Consequently, the calculated autotrophic index follows an increase over time in T20P16 conversely to the conditions T14P16 and T14P12 for which the autotrophic index slightly decreases (Figure 2C). In contrast, studied light and temperature conditions had no effect on the biofilm photosynthetic efficiency during the 7 days of exposure (Figure 2D). The average values were 0.46 ± 0.01 for T14P16, 0.44 ± 0.02 for T14P12 and 0.43 ± 0.02 for T20P16 (relative scale) with no apparent trends.

As mentioned in the materials and methods section, the biofilm was collected from the Cap-Rouge River and was then inoculated and cultured for one month in a culture channel. The different experiments were then carried out successively, leaving a two-week period between each experiment in order to modify the environmental conditions and acclimate the biofilm. The biofilm used in condition T20P16 was thus grown for a longer period of time than the biofilms studied in the conditions T14P16 and T14P12 (approximately 45 days and 21 days longer, respectively). It follows that the biofilm used in condition T20P16 had higher total Chl-a and dry weight biomass than those used in T14P16 and T14P12. This change may have affected the community structure and its response to Ni. In summary, abiotic conditions affected the community structure and different community structures might show different sensitivity to Ni. Note that a difference of 4 hours in the photoperiod (T14P16 *vs* T14P12) did not have a significant effect on the same biomarkers in control biofilms.

Effects of temperature and light conditions on Ni-exposed biofilms

In Ni-exposed microcosms and by excluding the t_0 (*i.e.* day 0; before addition of Ni in the media), the mean calculated free Ni ion concentrations were 0.97 ± 0.51;

5.57 ± 0.71; 23.2 ± 2.4; 56.1 ± 0.3; 116 ± 6 μM (days 1, 4 and 7 combined; n = 12). A table showing the evolution of total and free Ni concentrations during exposure at different times is presented in supporting information (see Table S3). Statistical differences in free Ni concentrations were found between times and conditions for a same Ni concentration of exposure (ANOVA; p-value < 0.05). The differences found between sampling times for a given condition were due to evaporation losses with a slight increase in concentrations (about 10 to 16% depending the experiment). However, as suggested by the standard deviation, the calculated concentrations remained close to the desired concentrations.

Throughout the experiment and for each tested condition, the biomass in Ni-exposed microcosms remained stable or slightly increased during the 7 days of exposure with a more pronounced effect in the condition T20P16 (Figure 3A). Furthermore, despite no clear statistical differences, Chl-a concentrations appeared to decrease over time in Ni-exposed microcosms (Figure 3B). This decrease was more pronounced in the T14P12 condition. Given the increase in biomass and decrease in Chl-a concentrations, the autotrophic index increased over time as for the controls (Figure 3C). However, the greater the exposure concentration was, the greater the increase in the autotrophic index was with a clear difference after 7 days of exposure. This increasing trend appeared only in conditions T14P16 and T14P12, the autotrophic index remaining relatively stable in condition T20P16.

Influence of the environmental conditions on Ni bioaccumulation

Ni accumulation by biofilms as a function of the free calculated Ni for the three environmental conditions is illustrated in Figure 4. At day 0 (*i.e.* before addition of Ni in any microcosm), the accumulated Ni concentrations remained within the same order of magnitude as those of the controls (values ranging from 0.3 to 1.6 μmol/g

dw). Indeed, for each condition tested, and except for one sample found as an outlier using the interquartile range approach (condition T14P12 for microcosms defined as $[Ni^{2+}] = 115$ µM at day 0; $[Ni]_{Bio} = 3.9$ µmol/g dw), no statistical differences were found between the accumulated Ni concentrations between each channel on day 0.

If we first compare the two photoperiods, Ni accumulation in biofilms increased with exposure concentrations up to 25 µM of Ni^{2+} for the three Ni-exposure sampling times (Figure 4; respectively panels A, B, C for days 1, 4 and 7). At higher Ni concentrations (55 and 115 µM), the accumulated Ni contents remained similar with average values below 30 µmol/g dw and this trend was observed at each sampling time. Note that the Ni exposure concentrations remained constant over time (see supporting information; Table S3). The Ni accumulation peaked after the first day of exposure, regardless of the exposure concentrations, with little to no increase at days 4 and 7. Only the 115 µM of Ni^{2+} treatment was significantly different over the three sampling times (*i.e.* day 1, 4 or 7). This difference leads to statistically different *Vm* estimates of the Michaelis-Menten models between day 1 and days 4 and 7 (see supporting information for the statistics between sampling times; Table S5). Nevertheless, biofilms exposed with a 12/12 photoperiod tend to globally have higher average internalized Ni concentrations than biofilms exposed with a 16/8 photoperiod as shown by the statistical difference found between the two calculated *Vm* (Table 1).

If we now compare the two tested temperatures, similar accumulation patterns were found for both conditions. Regardless of the Ni concentrations, the biofilm exposed at a temperature of 20°C showed an increasing internalized Ni content between days 1 and 4, and a plateau reached beyond day 4. Biofilms grown at 20°C and exposed to Ni systematically showed a significantly higher Ni accumulation for exposure concentrations greater than 1 µM. When all sampling times are pooled

together, the average internalized Ni at 20°C were higher by a factor ranging from 1.6 to 4.2. Indeed, the estimate of the parameter Vm shows a strong increase compared to the other conditions ($Vm = 32.0 \pm 4.5$ for T14P16; $Vm = 24.0 \pm 4.1$ for T14P12 and $Vm = 92.3 \pm 5.0$ in the case of T20P16).

Influence of temperature and light on Ni toxicity

Dose-response curves were fitted using the PSII efficiency as a function of the free Ni^{2+} concentrations. Their respective EC10, EC20 and EC50 were estimated with 95% confidence intervals for each environmental condition (Figure 5). The photosynthetic yield was found to be affected by the concentration of Ni^{2+} and the effect increased with exposure time. Regardless of the sampling time considered, the curves show a decreasing trend starting from a concentration of 5 µM. However, the maximum percentages of inhibition (compared to the control) were between $16 – 25$ %, $36 – 51$ % and $53 – 65$ % for days 1, 4 and 7, respectively. These results demonstrate the chronic toxicity of Ni over time on the photosynthetic efficiency of biofilms. For condition T20P16, the curves at 4 and 7 days are very close to those obtained for T14P16 and T14P12 where the toxic effect over time is more gradual. However, the PSII efficiency was negatively correlated with the bioaccumulated Ni ($R^2 = 0.33$, p-value < 0.001). Correlation coefficients calculated for each condition separately increased as follows: T14P12 ($R^2 = 0.22$; p-value < 0.001) < T14P16 ($R^2 = 0.32$; p-value < 0.001) < T20P16 ($R^2 = 0.51$; p-value < 0.001). The stronger correlation observed in condition T20P16 could be attributed to the greater bioaccumulation described above. Based on the final sampling time (day 7), calculated EC50s were statistically different between conditions T14P16, T14P12 or T20P16 (t test; p < 0.05). Calculated EC50 values for each condition increased as

follows: T20P16 < T14P12 < T14P16. Thus, phototrophic biofilm exposed at 20°C showed a lower tolerance to Ni in comparison to those exposed at 14°C.

Interaction between environmental factors and biofilm parameters

A LDA was carried out with all the measured biological parameters and Ni^{2+} concentrations for the day 7, and condition T20P16 was well discriminated (data not shown). This finding is consistent with the results described above, as the different descriptors have shown similar responses for conditions T14P16 and T14P12. However, Figure 6 presents an LDA performed with data obtained at day 7 of the exposure normalized for the respective starting conditions (i.e. day 7 / day 0) in order to consider the observed differences of the communities from the first sampling time (i.e. day 0). Based on this normalization, the three environmental conditions are not clearly discriminated. These results suggest that environmental conditions affected the community during the acclimation phase (and thus before the Ni exposure) and that this effect led, at least partially, to a difference in Ni responses of biofilms.

DISCUSSION

Ni effect on biofilm

Despite the fact that Chl-a concentrations and dry weight biomass were much lower at 14°C in comparison to those at 20°C, similar trends were found between both parameters in Ni-exposed biofilms (Figure 3). Biomass and Chl-a concentrations were observed to slightly increase and decrease, respectively, over time. The toxic effects of Ni observed in this study are in accordance with those found in the literature on biofilms and other microorganisms, and with other metals in general. Ni has been shown to negatively affect biofilm function by reducing Chl-a concentrations or the primary net production (Costello & Burton, 2014) such as biofilm structure with the disappearance of cyanobacterial populations (Lawrence et al., 2004). Fechner et al.

(2011), who exposed biofilms to low (0.09 μM) and high (0.85 μM) dissolved Ni

treatments, showed low variations of both dry weight biomass and Chl-a. However

important changes in both bacterial and eukaryotic communities were also observed.

In addition, the new metabarcoding approach has allowed for the observation of

significant changes in eukaryote and prokaryote community compositions along a

coastal sediment Ni concentration gradient (Gillmore et al., 2021). More precisely,

these community changes were mainly correlated with the dilute- acid extractable

concentration of Ni in the sediments, which explained 26, 23, and 19% of the

variation for eukaryotes, diatoms, and prokaryotes, respectively. In the present study,

the autotrophic index of Ni-exposed biofilms increased with exposure time at 14°C.

Biofilm exposed to Ni at 20°C also showed an increasing trend, but values remained

relatively stable despite higher biomass and Chl-a values. If the senescence of algal

cells could not be excluded especially at high Ni concentrations, this could also be due

to a modification of the assemblage in favour of heterotrophic organisms. Ancion et

al. (2010) exposed biofilms to different urban runoff treatments containing metal

mixtures of Zn, Cd and Cu during short (5 days) and long term (21 days) experiments.

The authors found significant differences in bacterial community structure occurring

after only 3 days of treatment confirming the rapid and sensitive reactivity of

microbial populations to metal exposure. Additionally, it is well known that chronic

exposures to metals (i.e. alone or in mixture) result in effects on bacterial community

structures (Medley & Clements, 1998; Tlili et al., 2011; Wolff et al., 2021). Our

results are in agreement with this previous work as the autotrophic index slightly

increased after 7 days and above the first exposure concentration (1 μM of Ni^{2+};

Figure 3).

In addition, a concentration of 25 μM of Ni^{2+} was found to have a significant inhibitory effect on photosynthetic processes, consequently impeding CO_2 fixation, as has been previously observed with other metals such as Cu and Zn (Figure 5; Corcoll et al., 2011; Lambert et al., 2017). Indeed, above this threshold concentration, Ni toxicity affected photosynthetic efficiency, and its resultant impact increased over time, demonstrating long-term effects (Figure 5). Conversely, for lower concentrations, the absence of significant effect resulting from Ni exposure on photosynthetic efficiency suggests that Ni did not drastically affect the algal physiologic state. Interestingly, the amount of internalized Ni increased with exposure to free Ni^{2+} concentrations up to a threshold concentration of 25 μM, at which point accumulation reached a plateau. At higher concentrations (*e.g.* 55 and 115 μM of Ni^{2+}; Figure 4), internalization was no longer dependent on exposure concentration, likely due to the Ni-induced toxicity on the phototrophic compartment. Although the results of T14P16 and T14P12 could suggest the saturation of Ni transporters, the data obtained in T20P16 indicate an abrupt decrease in uptake at the highest tested Ni concentration (*e.g.* 115 μM of Ni^{2+}) which is more consistent with a toxic effect than a saturation effect. In other words, these results suggest that Ni-induced toxicity explains the plateau observed for internalized concentrations for exposures greater than 25 μM of Ni^{2+} and this, from the first time of exposure. Similar conclusions were reached in biofilms exposed for 28 days to different Ni concentrations (dissolved concentrations ranging from 5.5 μM to 105 μM) at 15 and 21°C (Fadhlaoui et al., 2020). Accumulated Ni increased with Ni exposure concentration, with the highest internal values observed at 25 μM Ni^{2+}, followed by a marked decrease above this exposure concentration. In fact, nickel toxicity may induce direct and indirect effects, with the observed phototrophic cellular death possibly explaining the observed plateau

in metal bioaccumulation, which could subsequently increase available organic matter as nutrient for the heterotrophic compartments (Massieux et al., 2004; Boivin et al., 2005). If metals were to interfere with the functioning of heterotrophs (Fechner et al., 2011; Pesce et al., 2018), changes in the structure and diversity of the community towards more tolerant species could also rapidly occur (Ancion et al., 2010; Tlili et al., 2011; Morin et al., 2017). Furthermore, responses to Ni were quantifiable after 24 h of exposure, thus confirming the rapid, along with the high reactivity, of biofilms to metal exposure in terms of accumulation, information of particular importance for future impact assessments.

Influence of temperature and light variations on metabolism

Intra-daily or seasonal variation of conditions in natural environments can occur and are likely to influence the sensitivity of microbial communities to contaminants. For instance, Villeneuve et al. (2010) observed that light intensity or hydrodynamic conditions affect the structure and diversity of river biofilms. Variations in environmental factors are well-known phenomena that make difficult the establishment of relationships between metal exposure and the observed biological effects (Bonet et al., 2013; Faburé et al., 2015; Lambert et al., 2017). In our study, while photoperiod had no significant effect on the growth of biofilms unexposed to Ni, biofilm formation was more productive at high temperature (see Figure 2 and Figure 3). An increase in temperature is known to favour the metabolism of organisms such as bacteria and algae (Lürling et al., 2013). Additionally, several microcosm studies found that an increasing temperature influenced global phototrophic community structure, both in terms of algal biomass and in terms of the distribution of main algal classes. For instance, the structural parameters of periphytic microalgal communities (*e.g.* cell densities such as Chl-a content per cm^2) were affected by

temperature, especially above 21°C among the four tested temperatures (18, 21, 24 and 28°C; Larras et al., 2013). In this study, the authors observed a decrease in diatom diversity in periphyton communities between different temperature treatments, highlighting the dependence of biofilm communities on seasonal and environmental characteristics. Similar conclusions were reached by Lambert et al. (2016) and Morin et al. (2017). Both studies demonstrated that an increase of temperature led to a shift in diatom assemblage composition with a strong decrease in diversity leading to a modification of the community tolerance towards Cu. Furthermore, the lack of significant effect of temperature on the photosynthetic efficiency of control phototrophic communities suggests that the experimental warming did not drastically affect the physiologic state of phototrophic organisms within the biofilm studied. If photosynthetic activity is directly related to metabolism, which is dependent upon temperature, a difference of 6°C did not seem to be sufficient to observe a significant difference. These results are in agreement with several studies which found no effect on the maximum PSII quantum yields (Larras et al., 2013; Pesce et al., 2018; Chaumet et al., 2020). However, some discrepancy was found, for example in a study examining the effect of a 10°C temperature rise (18°C and 28°C) on the tolerance to Cu for phototrophic biofilm (Lambert et al., 2017). Indeed, a significant decrease was observed in PSII values for control biofilms at 28°C (in comparison to 18°C), which revealed an inhibitory effect of temperature on photosynthesis. These results highlighted the importance of the initial taxonomic composition and/or the difference in the temperature gradients tested. Concerning heterotrophic organisms, temperature is known to promote bacterial growth and exopolysaccharide (EPS) production (Boivin et al., 2005; More et al., 2014), which has been demonstrated in the field (Faburé et al., 2015). A warming stress was observed to have a significant influence

on extracellular enzymatic activity such as the β-glucosidase, an enzyme involved in carbon degradation, suggesting that the metabolism of organisms such as bacteria and fungi were enhanced (Pesce et al., 2018; Chaumet et al., 2020). Our findings are therefore in agreement with an increase of the autotrophic index at 20°C in control biofilms. Although the LDA was not able to discriminate the influence of the two temperatures when parameters were normalized by their respective conditions at day 0, the two conditions seems to dissociate along the x-axis which was related to the amplitude of variation in the autotrophic index (Figure 6).

Among the light components and as mentioned by Cheloni & Slaveykova (2018), most of the studies dealing with light effects focused on ultra violet radiation (within the spectrum of UVA or UVB), while the understanding of the role of the photosynthetically active radiation (PAR) and solar light in trace metal effects was overlooked. Based on our data, we found no evidence that photoperiod is as critical as temperature. Chaumet et al. (2020), who exposed biofilms in microcosms to two photoperiods (16/8 and 10/14 light/dark cycle) and two temperatures (10 and 26°C), found an interaction between the influence of both parameters. The study highlights the influence of temperature but also photoperiod on biofilm metabolism and, in particular, the parameters related to heterotrophic organisms (*i.e.* polysaccharide and protein content, and β-glucosidase activity). However, the two photoperiods were not clearly discriminated in our LDA analysis although they seem to dissociate along the y-axis principally related to Chl-a (Figure 6). This suggests that a light/dark cycle of 12/12 may also have an influence by being beneficial for heterotrophic organisms in comparison to 16/8. This result is important if Ni toxicity is dependent upon either autotrophic or heterotrophic organisms, should one be more affected than the other, there is the potential for additive/synergistic effects caused by Ni exposure and

photoperiod. As biofilms are composed of highly interconnected microorganisms (Battin et al., 2016), a strong effect on one compartment could generate an indirect effect on the other, thus leading to structural and functional changes. On the other hand, in terms of photosynthetic yield, Chaumet et al. (2020) found no marked effects of photoperiod, regardless of exposure time. It thus appears that photoperiod is not more influential as an external stress when compared to temperature. However, Corcoll et al. (2012) evaluated in a microcosm the relationship between short-term light intensity changes on the toxicity of Zn to fluvial biofilms with different photo-acclimation. Depending on the treatment, biofilms were characterized by different structural (Chl-a, dry-weight biomass, EPS, algal groups/taxonomy) and physiological attributes (photosynthetic pigments). The sensitivity of biofilms exposed to a multi-stress situation (*i.e.* sudden change in light intensity and Zn exposure) varied according to photo-acclimation pre-treatments. Furthermore, light intensity has been shown to be one of the environmental factors which determined the seasonality of biofilm responses in the field (Bonet et al., 2013). Therefore, it would appear that light intensity and spectral composition are more important than the photoperiod in regards to the capacity of biofilm to tolerate metal exposure.

Interactions between environmental factors, nickel toxicity and accumulation

The effects of environmental factors on Ni toxicity were significant in the case of temperature. The calculated *Vm* in this study confirmed an interaction between Ni bioaccumulation and temperature (as well as for the photoperiod although less marked (Table 1). Interestingly, these results suggest that metal accumulation in natural systems may vary with these two parameters. In addition, temperature modulated the functional effects of Ni, as shown by the measured photosynthetic efficiency values in Ni-exposed biofilms. Calculated EC50s using the Φ_{PSII} after 7 days showed statistical

differences between the three conditions with a decreasing trend in toxicity as follows: T14P16 < T14P12 < T20P16 (Figure 5). Biofilms exposed to 20°C accumulated higher levels of Ni (*i.e.* 1.6 to 4.2-fold higher at 20°C; Figure 4), which is in accordance with the lower EC50 in that condition (Figure 5). Our EC50 values are higher than those published for microalgae (Deleebeeck et al., 2009; Binet et al., 2018; Macoustra et al., 2021). For instance, Macoustra et al. (2021) found an EC50 for *Chlorella sp*. of 2 μM of Ni (72-h toxicity test), for a free nickel concentration of 0.43 μM in their exposure media. Based on published species sensitivity distributions (SSDs) for nickel, these results suggest that biofilm sensitivity to nickel is lower than microalgae, microalgae being placed relatively midway along the SSD for nickel after invertebrates (e.g., gastropods, crustaceans, and echinoderms; Stauber et al., 2021). Although Ni sensitivity of aquatic organisms varies between taxonomic groups, habitat, physico-chemistry of the media, our results suggest that abiotic parameters such as temperature variations should be considered in risk assessment.

Overall, biofilm appeared to be more impacted by Ni and more productive at 20°C than at 14°C. However, using all descriptors, the LDA could not clearly discriminate the temperature condition from the others (see Figure 6). Nevertheless, these results highlight the influence of temperature on the metabolism of the phototrophic component of the biofilm and illustrate the previous conclusions that this factor influenced Ni accumulation and thus, the Ni sensitivity of biofilms. However, because temperature affected the community structure during the acclimatization phase resulting in observable differences from day 0, the temperature might have directly or indirectly modified Ni sensitivity of the two biofilms exposed at 14 or 20 °C. This is in agreement with studies that found an influence of temperature on the vulnerability of phototrophic and heterotrophic microbial communities to metal toxicity (Lambert

et al., 2016; Lambert et al., 2017; Pesce et al., 2018). All these studies showed that a temperature increase modulates the response of biofilm to chronic Cu exposure depending on the function considered (*i.e.* phototrophic or heterotrophic organisms).

To our knowledge, in any previous efforts made to understand the link between tolerance acquisition and taxonomic composition of the community to metal exposure, few studies have closely investigated bioaccumulation. For instance, Friesen et al. (2017) utilized microcosms to expose natural biofilm of the same inoculum to Se for 21 days under different light and nutrient conditions. The authors found that the different environmental conditions tested resulted in different taxonomic composition within biofilms, but also significant differences in internalized Se concentrations. Their findings suggest that factors other than total dissolved Se concentration in the water influence Se accumulation in the biofilm, including taxonomic composition and physicochemical characteristics of the water. Lambert et al. (2016) and Pesce et al. (2018) exposed biofilms to Cu using similar methods to the current study and found that internalized Cu tended to decrease with increasing temperature, albeit statistically non-significant. However, Cu speciation is known to be highly sensitive to pH and organic ligands (*e.g.* dissolved organic matter, algal exudates) and only a small proportion of Cu is usually present as the free ion (Mueller et al., 2012; Macoustra et al., 2020). If authors emphasized that this reduction of Cu bioaccumulation was not due to a limitation of dissolved Cu concentrations, they also mentioned the possibility of a difference in exposure due to Cu bioavailability. If dissolved organic matter is also known to play a role in Ni speciation (Macoustra et al., 2021), using free metal concentrations, as in this study, ensures that the approach can be generalized to various water chemistry conditions, thus allowing a better lab-to-field extrapolation. However, based on total nickel concentrations, our results are in agreement with

previous studies that found biofilm Ni content around 1000 μg/g dw for total

concentrations above 25 μg/L (Hommen et al., 2016; Mebane et al., 2020). To our

knowledge, only Fadhlaoui et al. (2020) exposed biofilms to Ni in microcosms at

different temperatures. These authors found no apparent differences in accumulated

Ni between the two temperatures tested (15 and 21°C), contrasting with our results.

However, the range in accumulated metal was similar to that found in our study with

conditions T14P16 and T14P12 (around 40 μmol/g dw after 28 days of exposure).

Using confocal laser scanning microscopy (CLSM) and scanning transmission X-ray

microscopy (STXM), Lawrence et al. (2019) investigated Ni bioaccumulation and its

precise location within river biofilms. The authors showed that Ni was strongly

associated with EPS and that 4-fold more nickel was concentrated in specific

microcolonies than in overall biofilms. As a comparison Se was shown to be

associated with protein and polysaccharide biofilm components (Yang et al., 2016).

Findings also suggest an important role for specific community members in the

sorption and concentration of Ni (and more generally metals such as Se) in aquatic

biofilm communities. It could be hypothesized that the structure of the biofilm, such

as the taxonomic composition, may explain the differences of accumulation found in

this study based on the idea that specific temperatures are more favourable for some

organisms. This hypothesis could explain the higher bioaccumulation of biofilms

exposed at 20°C compared to those exposed at 14°C. From this perspective, using

community-based approaches, such as metabarcoding, while investigating

bioaccumulation as a function of the free metal ion concentration would provide

important information about how internalized metal concentrations are being affected

by taxonomic community composition or specific organisms (Gillmore et al., 2021).

Our results are coherent with those published in a previous field study (Laderriere et al., 2021). Differences were found in the observed relationships between free metal ions and biofilm metal concentrations between two regions distanced 1700 km apart (northern and southern eastern Canada). The two regions were different in terms of climate, ecosystems and thus environmental conditions (*i.e.* temperature and photoperiod). The southern biofilm showed higher internalized concentrations of metals studied (Cu, Ni and Cd) for the same concentration of free metal ions in ambient water as compared to the northern biofilms. Our results suggest that temperature plays an important role in the bioaccumulation of metals by the biofilm and that this factor should be taken into account in the use of biofilm as a bio-indicator over large geographical scales.

CONCLUSIONS

Variability in environmental factors make it difficult to establish a causal link between metal exposure and observed biological effects. Furthermore, environmental conditions, which include high background metal concentrations could favour benthic microbial communities tolerant to metals. In this context, microcosm approaches are interesting because they allow us to study the influence of specific parameters while remaining at the community scale. In this study, the influence of interactions between environmental factors such as temperature and photoperiod, and Ni exposure on Ni bioaccumulation and toxicity were investigated. Nickel exposure caused a chronic effect on the efficiency of PSII, the percentage of inhibition increasing with the duration of exposure. On the other hand, Chl-a concentration values decreased when biomass increased over time for the different exposure concentrations. This suggests that the heterotrophic compartment was less impacted than the phototrophic one. Furthermore, our results suggest that temperature has a stronger effect on Ni

accumulation than photoperiod. Indeed, biofilms exposed at a temperature of 20°C bioaccumulated more Ni than those exposed at 14°C for a given exposure concentration and were characterized by a lower EC50 value. This greater sensitivity could be due to higher intracellular Ni concentrations resulting in a lower ability of organisms to regulate their Ni content. This suggests that temperature influenced directly (*e.g.* by influencing cell metabolism) or indirectly (*e.g.* by modifying biofilm structure/composition) and thus, modified the Ni sensitivity of biofilms. In a context where freshwater biofilms may be used as indicators of metal exposure, these results imply that seasonal variations in the bioaccumulation response of metals is likely to occur.

Further studies should focus on the different functional compartments (*e.g.* phototrophic and heterotrophic) of biofilms by using descriptors to assess interactive effects of multiple stressors at the community level. Indeed, it would be interesting to explore Ni toxicity in the heterotrophic compartment of biofilms to examine if the vulnerability of microbial communities to subsequent Ni exposure depends on the studied function. In order to allow extrapolation of laboratory data to the natural environment, it appears crucial to understand the links between bioaccumulation, changes in environmental conditions and the taxonomic community composition of freshwater biofilms.

REFERENCES

Ancion, P. Y., Lear, G., & Lewis, G. D. (2010). Three common metal contaminants of urban runoff (Zn, Cu & Pb) accumulate in freshwater biofilm and modify embedded bacterial communities. *Environmental Pollution*, *158*(8), 2738–2745. https://doi.org/10.1016/j.envpol.2010.04.013

Battin, T. J., Besemer, K., Bengtsson, M. M., Romani, A. M., & Packmann, A. I. (2016). The ecology and biogeochemistry of stream biofilms. *Nature Reviews Microbiology*, *14*(4), 251–263. https://doi.org/10.1038/nrmicro.2016.15

Binet, M. T., Adams, M. S., Gissi, F., Golding, L. A., Schlekat, C. E., Garman, E. R., Merrington, G., & Stauber, J. L. (2018). Toxicity of nickel to tropical freshwater and sediment biota: A critical literature review and gap analysis. *Environmental Toxicology and Chemistry*, *37*(2), 293–317. https://doi.org/10.1002/etc.3988

Boivin, Y., Massieux, B., Breure, A. M., Ende, F. P. Van Den, Greve, G. D., Rutgers, M., & Admiraal, W. (2005). Effects of copper and temperature on aquatic bacterial communities. *Aquatic Toxicology*, *71*, 345–356. https://doi.org/10.1016/j.aquatox.2004.12.004

Bonet, B., Corcoll, N., Acuña, V., Sigg, L., Behra, R., & Guasch, H. (2013). Seasonal changes in antioxidant enzyme activities of freshwater biofilms in a metal polluted Mediterranean stream. *Science of the Total Environment*, *444*, 60–72. https://doi.org/10.1016/j.scitotenv.2012.11.036

Bonnineau, C., Artigas, J., Chaumet, B., Dabrin, A., Faburé, J., Ferrari, B. J. D., Lebrun, J. D., Margoum, C., Mazzella, N., Miège, C., Morin, S., Uher, E., Babut, M., & Pesce, S. (2020). Role of biofilms in contaminant bioaccumulation and trophic transfer in aquatic ecosystems: current state of knowledge and future challenges. *Reviews of Environmental Contamination and Toxicology*, *253*, 115–153. https://doi.org/10.1007/398_2019_39

Chaumet, B., Mazzella, N., Neury-Ormanni, J., & Morin, S. (2020). Light and temperature influence on diuron bioaccumulation and toxicity in biofilms. *Ecotoxicology*, *29*(2), 185–195. https://doi.org/10.1007/s10646-020-02166-8

Chaumet, B., Morin, S., Hourtané, O., Artigas, J., Delest, B., Eon, M., & Mazzella, N. (2019). Flow conditions influence diuron toxicokinetics and toxicodynamics in freshwater biofilms. *Science of the Total Environment*, *652*, 1242–1251. https://doi.org/10.1016/j.scitotenv.2018.10.265

Cheloni, G., & Slaveykova, V. I. (2018). Combined effects of trace metals and light on photosynthetic microorganisms in aquatic environment. *Environments*, *5*(81), 1–19. https://doi.org/10.3390/environments5070081

Corcoll, N., Bonet, B., Leira, M., & Guasch, H. (2011). Chl-a fluorescence parameters as

biomarkers of metal toxicity in fluvial biofilms: An experimental study. *Hydrobiologia*, *673*(1), 119–136. https://doi.org/10.1007/s10750-011-0763-8

Corcoll, N., Bonet, B., Leira, M., Montuelle, B., Tlili, A., & Guasch, H. (2012). Light history influences the response of fluvial biofilms to Zn exposure. *Journal of Phycology*, *48*(6), 1411–1423. https://doi.org/10.1111/j.1529-8817.2012.01223.x

Corcoll, N., Bonet, B., Morin, S., Tlili, A., Leira, M., & Guasch, H. (2012). The effect of metals on photosynthesis processes and diatom metrics of biofilm from a metal-contaminated river: A translocation experiment. *Ecological Indicators*, *18*, 620–631. https://doi.org/10.1016/j.ecolind.2012.01.026

Costello, D. M., & Burton, G. A. (2014). Response of stream ecosystem function and structure to sediment metal: Context-dependency and variation among endpoints. *Elementa*, *2*, 1–13. https://doi.org/10.12952/journal.elementa.000030

Deleebeeck, N. M. E., De Schamphelaere, K. A. C., & Janssen, C. R. (2009). Effects of Mg2+ and H+ on the toxicity of Ni2+ to the unicellular green alga Pseudokirchneriella subcapitata: Model development and validation with surface waters. *Science of the Total Environment*, *407*(6), 1901–1914. https://doi.org/10.1016/j.scitotenv.2008.11.052

Faburé, J., Dufour, M., Autret, A., Uher, E., & Fechner, L. C. (2015). Impact of an urban multi-metal contamination gradient: Metal bioaccumulation and tolerance of river biofilms collected in different seasons. *Aquatic Toxicology*, *159*, 276–289. https://doi.org/10.1016/j.aquatox.2014.12.014

Fadhlaoui, M., Laderriere, V., Lavoie, I., & Fortin, C. (2020). Influence of temperature and nickel on algal biofilm fatty acid composition. *Environmental Toxicology and Chemistry*, *39*(8), 1566–1577. https://doi.org/10.1002/etc.4741

Fechner, L. C., Gourlay-Francé, C., & Tusseau-Vuillemin, M. H. (2011). Low exposure

levels of urban metals induce heterotrophic community tolerance: A microcosm validation. *Ecotoxicology*, *20*(4), 793–802. https://doi.org/10.1007/s10646-011-0630-4

Flemming, H. C., & Wingender, J. (2010). The biofilm matrix. *Nature Reviews Microbiology*, *8*(9), 623–633. https://doi.org/10.1038/nrmicro2415

Friesen, V., Doig, L. E., Markwart, B. E., Haakensen, M., Tissier, E., & Liber, K. (2017). Genetic characterization of periphyton communities associated with selenium bioconcentration and trophic transfer in a simple food chain. *Environmental Science and Technology*, *51*(13), 7532–7541. https://doi.org/10.1021/acs.est.7b01001

Gillmore, M. L., Golding, L. A., Chariton, A. A., Stauber, J. L., Stephenson, S., Gissi, F., Greenfield, P., Juillot, F., & Jolley, D. F. (2021). Metabarcoding reveals changes in benthic eukaryote and prokaryote community composition along a tropical marine sediment nickel gradient. *Environmental Toxicology and Chemistry*, *40*(7), 1892–1805. https://doi.org/10.1002/etc.5039

Guasch, H., Artigas, J., Bonet, B., Bonnineau, C., Canals, O., & Corcoll, N. (2016). The use of biofilms to assess the effects of chemicals on freshwater ecosystems. In A. M. Romaní, H. Guasch, & M. D. Balaguer (Eds.), *In Aquatic Biofilms: Ecology, Water Quality and Wastewater Treatment* (pp. 125–144). Caister Academic Press, Spain. https://doi.org/10.21775/9781910190173.06

Harasim, P., & Filipek, T. (2015). Nickel in the environment. *Journal of Elementology*, *20*(2), 525–534. https://doi.org/10.5601/jelem.2014.19.3.651

Hassler, C. S., Slaveykova, V. I., & Wilkinson, K. J. (2004). Discrimination between intra- and extracellular metals using chemical extractions. *Limnology and Oceanography: Methods*, *2*, 237–247. https://doi.org/10.4319/lom.2004.2.237

Hobbs, W. O., Collyard, S. A., Larson, C., Carey, A. J., & O'Neill, S. M. (2019). Toxic

burdens of freshwater biofilms and use as a source tracking tool in rivers and streams. *Environmental Science and Technology*, *53*(19), 11102–11111. https://doi.org/10.1021/acs.est.9b02865

Hommen, U., Knopf, B., Rüdel, H., Schäfers, C., De Schamphelaere, K., Schlekat, C., & Garman, E. R. (2016). A microcosm study to support aquatic risk assessment of nickel: Community-level effects and comparison with bioavailability-normalized species sensitivity distributions. *Environmental Toxicology and Chemistry*, *35*(5), 1172–1182. https://doi.org/10.1002/etc.3255

Laderriere, V., Faucheur, S. Le, & Fortin, C. (2021). Exploring the role of water chemistry on metal accumulation in biofilms from streams in mining areas. *Science of the Total Environment*, *784*, 146986. https://doi.org/10.1016/j.scitotenv.2021.146986

Laderriere, V., Paris, L. E., & Fortin, C. (2020). Proton competition and free ion activities drive cadmium, copper, and nickel accumulation in river biofilms in a nordic ecosystem. *Environments*, *7*(12), 1–13. https://doi.org/10.3390/environments7120112

Lambert, A. S., Dabrin, A., Foulquier, A., Morin, S., Rosy, C., Coquery, M., & Pesce, S. (2017). Influence of temperature in pollution-induced community tolerance approaches used to assess effects of copper on freshwater phototrophic periphyton. *Science of the Total Environment*, *607–608*, 1018–1025. https://doi.org/10.1016/j.scitotenv.2017.07.035

Lambert, A. S., Dabrin, A., Morin, S., Gahou, J., Foulquier, A., Coquery, M., & Pesce, S. (2016). Temperature modulates phototrophic periphyton response to chronic copper exposure. *Environmental Pollution*, *208*, 821–829. https://doi.org/10.1016/j.envpol.2015.11.004

Larras, F., Lambert, A. S., Pesce, S., Rimet, F., Bouchez, A., & Montuelle, B. (2013). The effect of temperature and a herbicide mixture on freshwater periphytic algae.

Ecotoxicology and Environmental Safety, *98*, 162–170.

https://doi.org/10.1016/j.ecoenv.2013.09.007

Lavoie, I., Lavoie, M., & Fortin, C. (2012). A mine of information: Benthic algal

communities as biomonitors of metal contamination from abandoned tailings. *Science*

of the Total Environment, *425*, 231–241.

https://doi.org/10.1016/j.scitotenv.2012.02.057

Lavoie, I., Morin, S., Laderriere, V., & Fortin, C. (2018). Freshwater diatoms as indicators

of Combined long-term mining and urban stressors in Junction Creek (Ontario,

Canada). *Environments*, *5*(2), 30. https://doi.org/10.3390/environments5020030

Lawrence, J R, Chenier, M. R., Roy, R., Beaumier, D., Fortin, N., Swerhone, G. D. W.,

Neu, T. R., & Greer, C. W. (2004). Microscale and molecular assessment of impacts

of nickel, nutrients, and oxygen level on structure and function of river biofilm

communities. *Applied and Environmental Microbiology*, *70*(7), 4326–4339.

https://doi.org/10.1128/AEM.70.7.4326

Lawrence, John R., Swerhone, G. D. W., & Neu, T. R. (2019). Visualization of the sorption

of nickel within exopolymer microdomains of bacterial microcolonies using confocal

and scanning electron microscopy. *Microbes and Environments*, *34*(1), 76–82.

https://doi.org/10.1264/jsme2.ME18134

Leguay, S., Lavoie, I., Levy, J. L., & Fortin, C. (2016). Using biofilms for monitoring

metal contamination in lotic ecosystems: The protective effects of hardness and pH on

metal bioaccumulation. *Environmental Toxicology and Chemistry*, *35*(6), 1489–1501.

https://doi.org/10.1002/etc.3292

Lürling, M., Eshetu, F., Faassen, E. J., Kosten, S., & Huszar, V. L. M. (2013). Comparison

of cyanobacterial and green algal growth rates at different temperatures. *Freshwater*

Biology, *58*(3), 552–559. https://doi.org/10.1111/j.1365-2427.2012.02866.x

Macoustra, G. K., Jolley, D. F., Stauber, J. L., Koppel, D. J., & Holland, A. (2020). Amelioration of copper toxicity to a tropical freshwater microalga: Effect of natural DOM source and season. *Environmental Pollution*, 115–141. https://doi.org/10.1016/j.envpol.2020.115141

Macoustra, G. K., Jolley, D. F., Stauber, J. L., Koppel, D. J., & Holland, A. (2021). Speciation of nickel and its toxicity to Chlorella sp. in the presence of three distinct dissolved organic matter (DOM). *Chemosphere*, *273*, 128454. https://doi.org/10.1016/j.chemosphere.2020.128454

Massieux, B., Boivin, M. E. Y., Van Den Ende, F. P., Langenskiöld, J., Marvan, P., Barranguet, C., Admiraal, W., Laanbroek, H. J., & Zwart, G. (2004). Analysis of structural and physiological profiles to assess the effects of Cu on biofilm microbial communities. *Applied and Environmental Microbiology*, *70*(8), 4512–4521. https://doi.org/10.1128/AEM.70.8.4512-4521.2004

Mebane, C. A., Schmidt, T. S., Miller, J. L., & Balistrieri, L. S. (2020). Bioaccumulation and toxicity of cadmium, copper, nickel, and zinc and their mixtures to aquatic insect communities. *Environmental Toxicology and Chemistry*, *39*(4), 812–833. https://doi.org/10.1002/etc.4663

Medley, C. N., & Clements, W. H. (1998). Responses of diatom communities to heavy metals in streams: The influence of longitudinal variation. *Ecological Applications*, *8*(3), 631–644. https://doi.org/10.1890/1051-0761(1998)008[0631:RODCTH]2.0.CO;2

Moe, S. J., De Schamphelaere, K., Clements, W. H., Sorensen, M. T., Van den Brink, P. J., & Liess, M. (2013). Combined and interactive effects of global climate change and toxicants on populations and communities. *Environmental Toxicology and Chemistry*, *32*(1), 49–61. https://doi.org/10.1002/etc.2045

More, T. T., Yadav, J. S. S., Yan, S., Tyagi, R. D., & Surampalli, R. Y. (2014).
Extracellular polymeric substances of bacteria and their potential environmental
applications. *Journal of Environmental Management*, *144*, 1–25.
https://doi.org/10.1016/j.jenvman.2014.05.010

Morin, S., Lambert, A. S., Rodriguez, E. P., Dabrin, A., Coquery, M., & Pesce, S. (2017).
Changes in copper toxicity towards diatom communities with experimental warming.
Journal of Hazardous Materials, *334*, 223–232.
https://doi.org/10.1016/j.jhazmat.2017.04.016

Mueller, K. K., Lofts, S., Fortin, C., & Campbell, P. G. C. (2012). Trace metal speciation
predictions in natural aquatic systems: Incorporation of dissolved organic matter
(DOM) spectroscopic quality. *Environmental Chemistry*, *9*(4), 356–368.
https://doi.org/10.1071/EN11156

Namba, H., Iwasaki, Y., Heino, J., & Matsuda, H. (2020). What to survey? A systematic
review of the choice of biological groups in assessing ecological impacts of metals in
running waters. *Environmental Toxicology and Chemistry*, *39*(10), 1964–1972.
https://doi.org/10.1002/etc.4810

Pesce, S., Lambert, A.-S., Morin, S., Foulquier, A., Coquery, M., & Dabrin, A. (2018).
Experimental warming differentially influences the vulnerability of phototrophic and
heterotrophic periphytic communities to copper toxicity. *Frontiers in Microbiology*,
9(July), 1424. https://doi.org/10.3389/fmicb.2018.01424

Serra, A., Guasch, H., Admiraal, W., Van Der Geest, H. G., & Van Beusekom, S. A. M.
(2010). Influence of phosphorus on copper sensitivity of fluvial periphyton: The role
of chemical, physiological and community-related factors. *Ecotoxicology*, *19*(4), 770–
780. https://doi.org/10.1007/s10646-009-0454-7

Stauber, J., Golding, L., Peters, A., Merrington, G., Adams, M., Binet, M., Batley, G.,

Gissi, F., McKnight, K., Garman, E., Middleton, E., Gadd, J., & Schlekat, C. (2021). Application of bioavailability models to derive chronic guideline values for nickel in freshwaters of Australia and New Zealand. *Environmental Toxicology and Chemistry*, *40*(1), 100–112. https://doi.org/10.1002/etc.4885

Steinman, A. D., Lamberti, G. A., & Leavitt, P. R. (2006). Biomass and pigments of benthic algae. In Elsevier (Ed.), *In: Methods in strem ecology* (Issue 3, pp. 357–379). https://doi.org/10.1016/b978-012332908-0.50024-3

Stewart, T. J., Behra, R., & Sigg, L. (2015). Impact of chronic lead exposure on metal distribution and biological effects to periphyton. *Environmental Science & Technology*, *49*(8), 5044–5051. https://doi.org/10.1021/es505289b

Tercier-Waeber, M.-L., Stoll, S., & Slaveykova, V. I. (2012). Trace metal behavior in surface waters: Emphasis on dynamic speciation, sorption processes and bioavailability. *Archives Des Sciences*, *65*(1–2), 119–142. https://archive-ouverte.unige.ch/unige:27739

Tlili, A., Corcoll, N., Arrhenius, Å., Backhaus, T., Hollender, J., Creusot, N., Wagner, B., & Behra, R. (2020). Tolerance patterns in stream biofilms link complex chemical pollution to ecological impacts. *Environmental Science and Technology*, *54*(17), 10745–10753. https://doi.org/10.1021/acs.est.0c02975

Tlili, A., Maréchal, M., Bérard, A., Volat, B., & Montuelle, B. (2011). Enhanced co-tolerance and co-sensitivity from long-term metal exposures of heterotrophic and autotrophic components of fluvial biofilms. *Science of the Total Environment*, *409*(20), 4335–4343. https://doi.org/10.1016/j.scitotenv.2011.07.026

Villeneuve, A., Montuelle, B., & Bouchez, A. (2010). Influence of slight differences in environmental conditions (light, hydrodynamics) on the structure and function of periphyton. *Aquatic Sciences*, *72*, 33–44. https://doi.org/10.1007/s00027-009-0108-0

Wolff, B. A., Clements, W. H., & Hall, E. K. (2021). Metals alter membership but not diversity of a headwater stream microbiome. *Applied and Environmental Microbiology*, *87*(7), 1–16. https://doi.org/10.1128/AEM.02635-20

Yang, S. I., George, G. N., Lawrence, J. R., Susan, G., Kaminskyj, W., Dynes, J. J., Lai, B., & Pickering, I. J. (2016). Multispecies biofilms transform selenium oxyanions into elemental selenium particles: studies using combined synchrotron X-ray fluorescence imaging and scanning transmission X-ray microscopy. *Environmental Science & Technology*, *50*(19), 10343–10350. https://doi.org/10.1021/acs.est.5b04529

FIGURE CAPTIONS
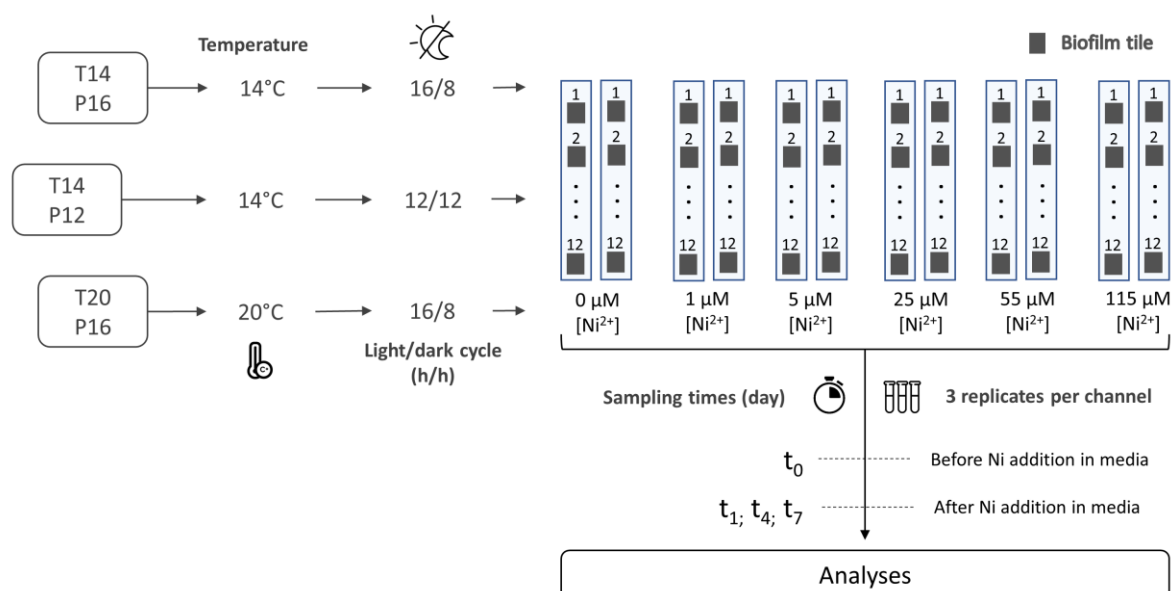
Figure 1: Graphical representation of the experimental design. The rectangles represent the microcosms and each square, a biofilm-covered tile. A total of 12 tiles were placed in each channel. Calculated free nickel ion concentrations [Ni^{2+}] are presented. The light intensity was maintained between 70 to 80 µmol·photon/m^2.
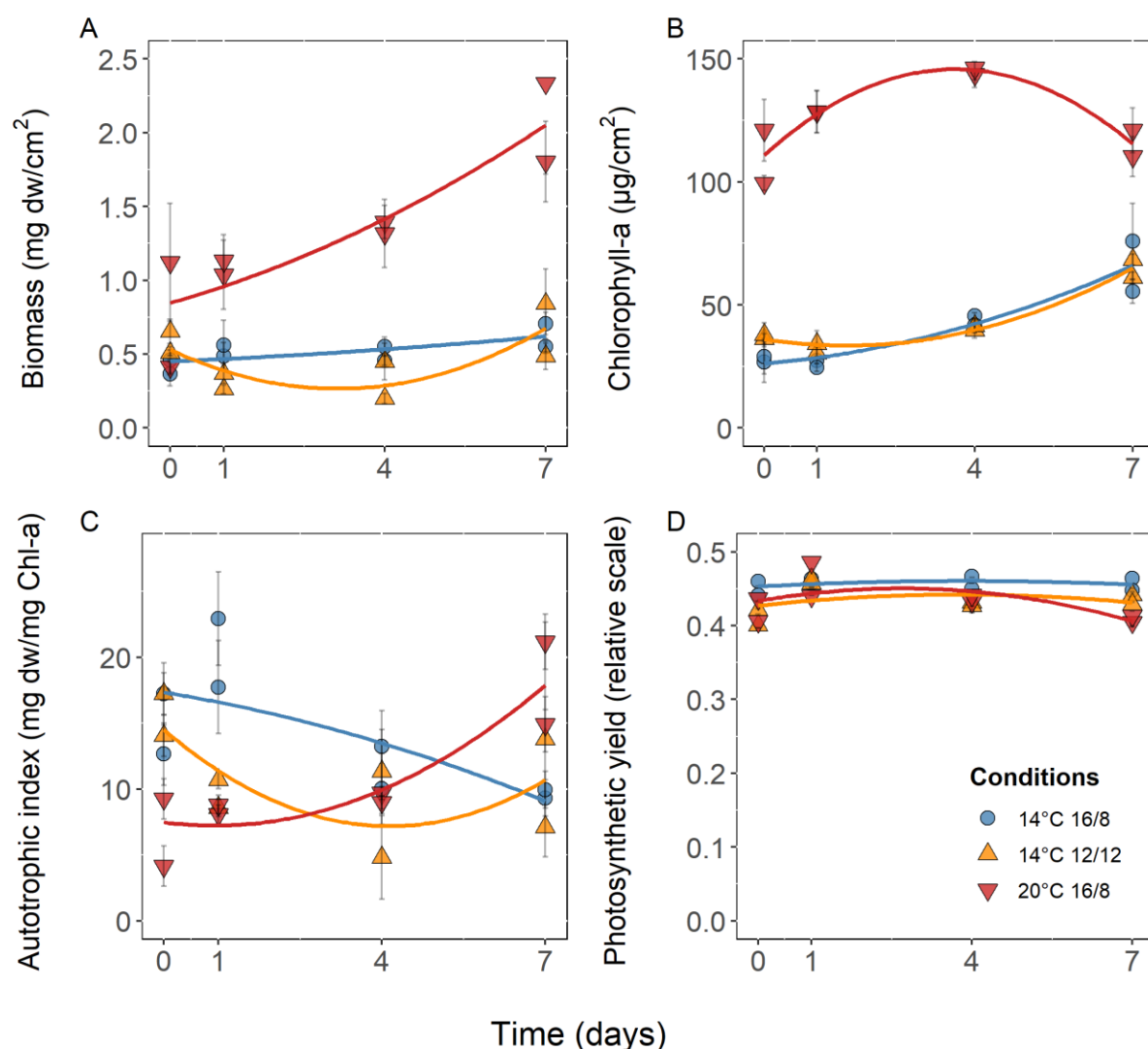
Figure 2: Time course of A) dry biomass, B) chlorophyll-a concentrations, C) autotrophic index and D) photosynthetic yield in control biofilms (each point represents the mean ± standard deviations of pseudo replicates; n = 3). In the case of condition T14P16 at day 7, Chl-a concentrations were estimated by regression using values obtained by Phyto-PAM and not by spectrophotometry. See materials and methods for more details. The curves drawn correspond to second-degree polynomial regressions using the two replicates (i.e. channel replicates of each Ni nominal concentrations tested) and are only intended to guide the eye of the reader. See supporting information for the results presented in table format (see Table S4).
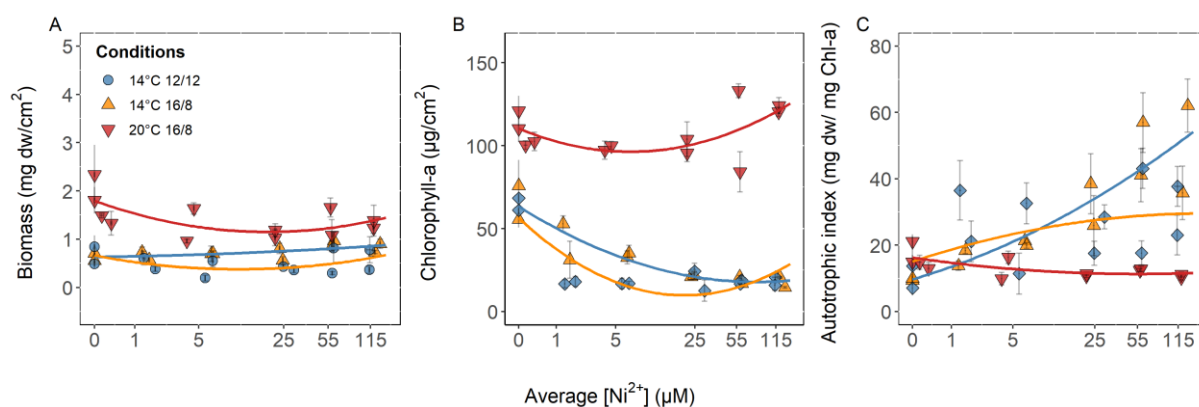
Figure 3: Dose responses of A) the biomass, B) the concentration of chlorophyll-a and C) the autotrophic index (n = 3) as a function of the free Ni concentration for each condition of temperature and photoperiod (T14P16 = 14°C in 16/8; T14P12 = 14°C in 12/12; and T20P16 = 20°C in 16/8). The curves plotted correspond to second-degree polynomial regressions using the two replicates (i.e. channel replicates of each Ni nominal concentrations tested) to guide the eye. A version of this figure with the data of each sampling times (i.e. day 1, 4 and 7) is presented in the supporting information (see Figure S2).
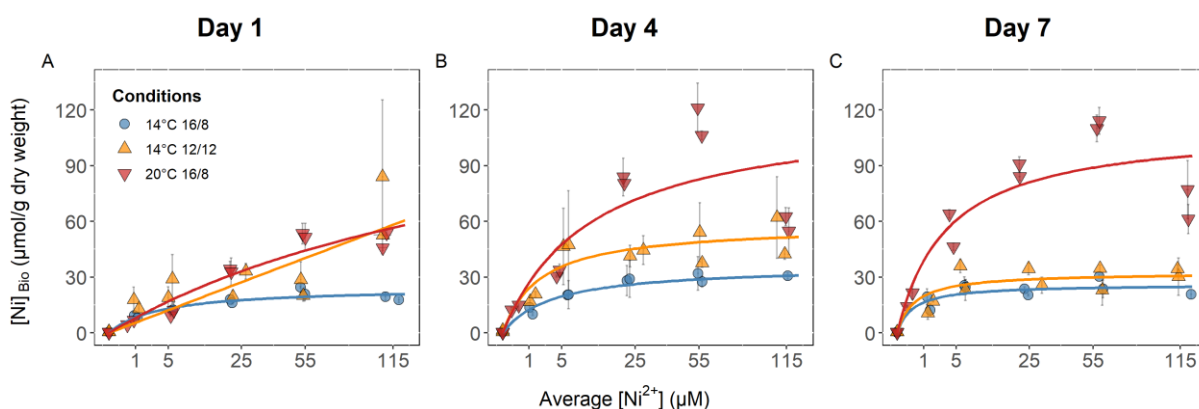

Figure 4: Internalized Ni concentrations by biofilms (n = 3 for the different conditions: 14°C and 16/8 light/dark cycle in blue; 14°C and 12/12 light/dark cycle in yellow; 20°C 16/8 light/dark cycle in red) as a function of the calculated free Ni concentrations at A) day 1, B) day 2 and C) day 3. The curves represent non-linear regressions using the Michaelis-Menten equation. The Ni accumulation of control

samples (non-exposed channels) ranged from 0.03 to 0.6 µmol/g dw over the entire
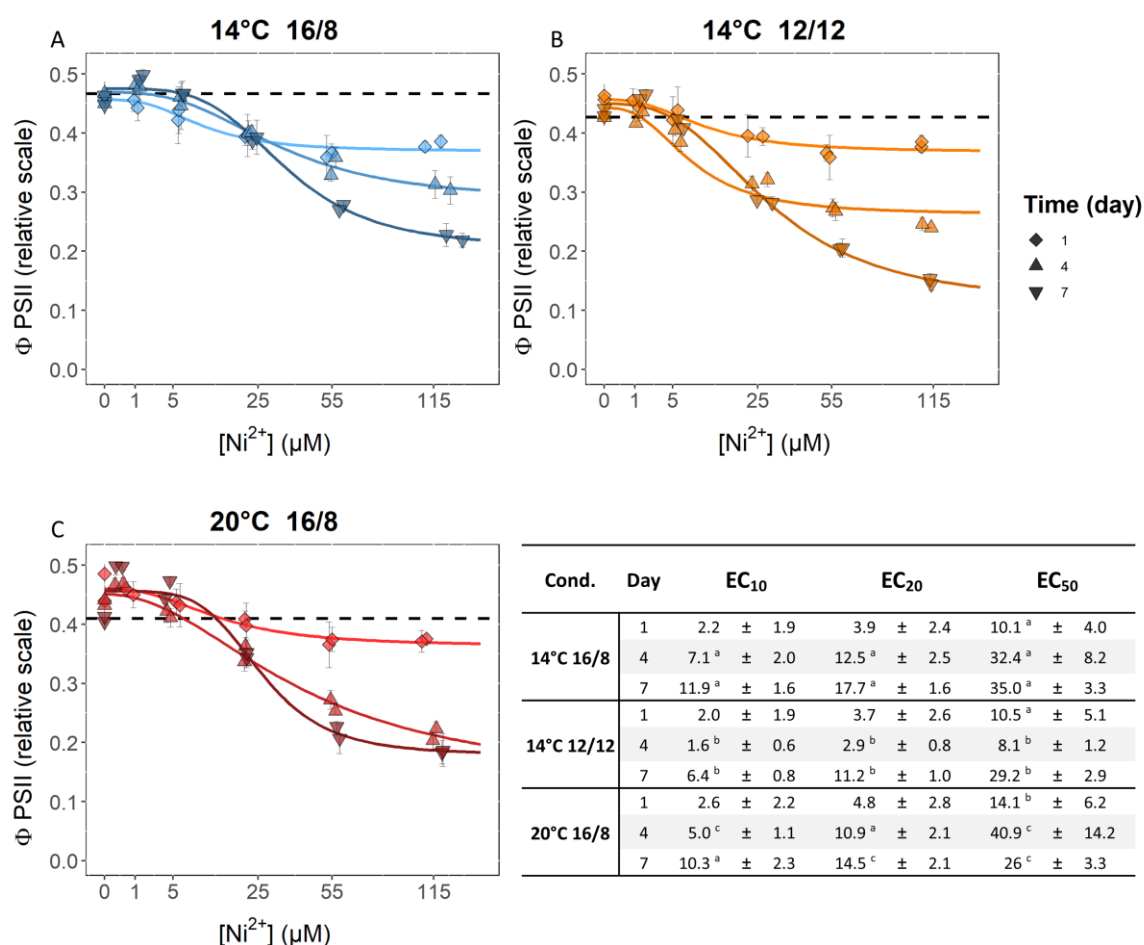
sampling period.

Figure 5: Photosynthesis efficiency as function of Ni^{2+} exposure for three

environmental tested conditions. Scatterplots show time-response of Φ_{PSII} after Ni

addition (mean ± SD; n = 3) at each exposure duration. Measurements of all t_0

samples (before addition of Ni in the media) were used as a reference to plot relative

dose-response curves. The dotted line shows the median value of the control samples.

Values of control samples (non-exposed channels) were comprised between 0.39 and

0.50 over the entire sampling period. A summary of the effective concentrations

calculated from each time curve is provided in the table for each condition (estimate ±

standard error). The letters indicate significant differences between conditions within
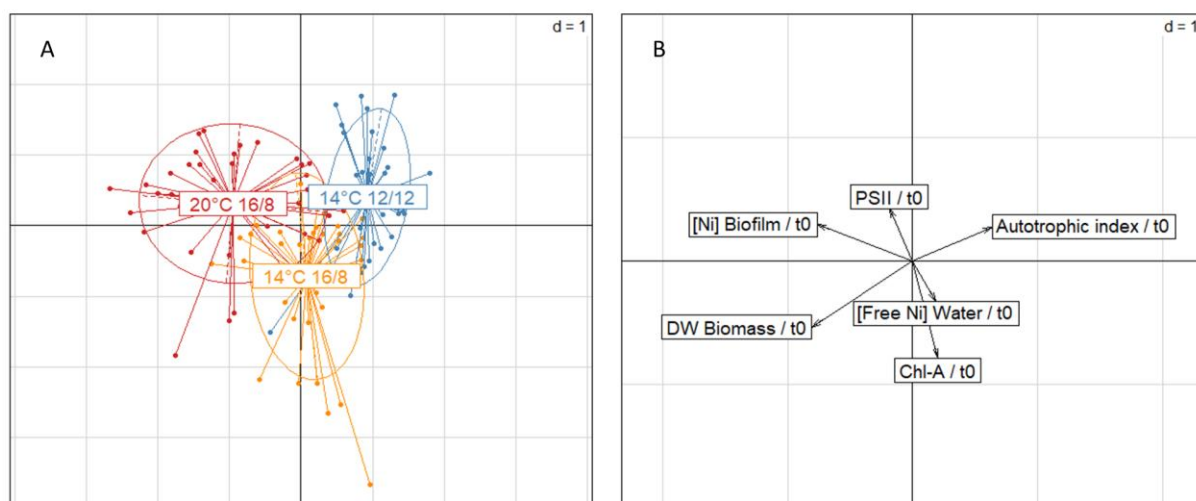
a same sampling time (p < 0.05).

Figure 6: Linear discriminant analysis (LDA) of the different conditions after the 7 days of exposure (A) based on the different studied biomarkers (B) for all Ni treatments. All the parameters were normalized based on their starting values (i.e. using their respective t_0 values) in order to discriminate the influence of environmental factors on response to Ni.

Table 1: Estimation of the coefficients of the Michaelis-Menten models for each environmental condition at the different exposure times. pwc = pairwise comparisons. n/a = not applicable (*i.e.* one or several estimates for the pairwise comparison are not significant).

Time (day)	Parameters	Conditions	Estimate	Std. Error	t-value	p-value	pwc
1	K	T14P16	330	491	0.67	0.51	n/a
		T14P12	2.1	2.8	0.75	0.46	
		T20P16	19	10	1.8	0.08	
	Vm	T14P16	266	313	0.85	0.4	n/a
		T14P12	20	4	4.5	$1.00e^{-04}$	a
		T20P16	63	10	6.1	$1.10e^{-06}$	b
4	K	T14P16	1.5	1.1	1.4	0.17	n/a
		T14P12	1.9	2.4	0.81	$4.20e^{-01}$	
		T20P16	5	2.2	2.3	0.03	
	Vm	T14P16	50	6	8.8	$9.00e^{-10}$	a
		T14P12	29	6	4.9	$2.80e^{-05}$	b
		T20P16	92	8	12	$6.40e^{-13}$	c
7	K	T14P16	1.5	1.4	1.1	0.28	n/a
		T14P12	0.58	0.93	0.63	0.54	
		T20P16	2.1	0.8	2.6	0.013	
	Vm	T14P16	32	5	7.1	$7.10e^{-08}$	a
		T14P12	24	4	5.9	$2.10e^{-06}$	b
		T20P16	92	5	18	$< 1e^{-16}$	c